water

MDPI

Article

Surface and Groundwater Characteristics within a Semi-Arid Environment Using Hydrochemical and Remote Sensing Techniques

Abdellatif Rafik [1,*], Mohammed Bahir [1,2], Abdelaziz Beljadid [1], Driss Ouazar [3], Abdelghani Chehbouni [1,4], Driss Dhiba [1] and Salah Ouhamdouch [2]

1 International Water Research Institute (IWRI), Mohammed VI Polytechnic University, Ben Guerir 43150, Morocco; bahir@uca.ac.ma (M.B.); Abdelaziz.BELJADID@um6p.ma (A.B.); Abdelghani.Chehbouni@um6p.ma (A.C.); Driss.DHIBA@um6p.ma (D.D.)
2 High Energy and Astrophysics Laboratory, Faculty of Sciences Semlalia, Cadi Ayyad University, Marrakech 40000, Morocco; salah.ouhamdouch@edu.uca.ma
3 Mohammadia School of Engineering, Mohamed V University, Rabat 10090, Morocco; driss.ouazar@um6p.ma
4 Centre D'études Spatiales de la Biosphère (Cesbio), Institut de Recherche Pour le Développement (IRD), Unité Mixte de Recherche (UMR), 31401 Toulouse, France
* Correspondence: abdellatif.rafik@um6p.ma; Tel.: +212-670-386-215

Abstract: The understanding of hydro systems is of great importance in monitoring quantitative and qualitative changes in water resources. The Essaouira region at the edge of the Moroccan Atlantic Ocean is subject to a semi-arid climate. The decrease in rainfall as a result of climate change and the increase in the exploitation of surface and groundwater have disrupted the stability of these resources and threaten the socio-economic and environmental balance in the area under investigation. Climate scenarios estimate that precipitation will decrease by 10–20% while warming increases by 3 °C over the next 30 years. The physico-chemical parameters studied show that the evolution of the pH and temperature of the groundwater remained stable with a neutral (pH ≈ 7) and a hypothermal character (T < 30 °C). For the electrical conductivity, it showed an increasing trend from 2017 to 2020. A hydrochemical approach showed that the groundwater mineralization was controlled by the dissolution of evaporites and carbonates, by cation exchange processes, and by seawater contamination. A groundwater assessment for drinking use was made by comparing the concentrations of the chemical elements with the standards set by the World Health Organization. The results obtained show that the groundwater from the aquifers studied requires treatment before being consumed, in particular for Cl^- and SO_4^{2-}. Furthermore, the groundwater quality for irrigation was evaluated based on the parameters Na% and Sodium Adsorption Ratio (SAR). The results showed that the groundwater was adequate for agricultural purposes, especially for the plants that adapt to high salinity. The monitoring of surface water by processing the satellite images via the calculation of the normalized difference water index (NDWI) showed an increase in water surface areas in the region following the commissioning of two large dams (Zerrar and Igouzoullene). Despite the installation of these hydraulic structures, a drop of 4.85 km^2 in water surface area was observed beyond 2016. This situation requires intervention in order to preserve this vital resource.

Keywords: groundwater; NDWI; water surface; semi-arid area; GIS

Citation: Rafik, A.; Bahir, M.; Beljadid, A.; Ouazar, D.; Chehbouni, A.; Dhiba, D.; Ouhamdouch, S. Surface and Groundwater Characteristics within a Semi-Arid Environment Using Hydrochemical and Remote Sensing Techniques. *Water* **2021**, *13*, 277. http://doi.org/10.3390/w13030277

Received: 20 December 2020
Accepted: 15 January 2021
Published: 24 January 2021

1. Introduction

In coastal environments in arid and semi-arid climates, groundwater pollution, including groundwater salinization, becomes a major topic since a series of circumstances favors the introduction of excess salts dissolved from different origins in these waters. The phenomenon of salinization is one of the main threats to groundwater in coastal areas [1–6]. This salinization is mainly due to the effects of climate change, marine intrusion, and agricultural and industrial activity [7–11].

Research on water resources indicates that Africa in general and Morocco in particular will reach an extremely high level of water stress by 2040. Water stress is the state that a region is in when its demand for water exceeds its available resources. According to the United Nations, Morocco is already classified as a water-stressed country, with only 786 m^3/inhabitant/year in 2020 according to estimates compared with 1044 m^3 in the 1990s, and a volume of 29 billion cubic meters per year that is renewable [12]. This decline is explained by population growth, lack of rationalization in the use of the resource, reduced rainfall due to climate change [13], and the ever-increasing natural aridity of certain regions of Morocco and many parts of Africa.

The Essaouira region on the Atlantic Ocean belongs to the arid and semi-arid climate zones of Morocco [14]. For the last three decades, the quality and availability of water resources in these areas have been negatively affected by climate change [9,15]. According to previous studies, the succession of drought cycles where the number of years of rainfall deficit exceeds the number of wet years [16,17] and the continuous increase in needs due to population growth and lifestyle improvements have negative consequences on the water resource potential. Climate change has a direct influence on water availability and quality in the Essaouira basin [16,17].

This study aimed to investigate and monitor the state and spatiotemporal evolution of surfaces and groundwater based on piezometric (quantitative behavior) and hydrochemical (qualitative behavior) approaches by using the results of the campaigns carried out in 2017, 2018, 2019, and 2020, as well as geographic information system (GIS) techniques. The results of this study will be used to allow for better management and protection of this vital resource.

2. Study Area

The study area, Essaouira Basin, is located on the Atlantic coastline of Morocco between latitudes 31.05° and 31.78° N and longitudes −9.06° and −9.84° W (Figure 1). Constituting the western end of the High Atlas Mountains, it covers an area of 3500 km^2 and contains 10% of the country's aquifers, namely, those of the Plio-Quaternary, Turonian, Cenomano-Turonian, and Hauterivian, whose structures and resources are often poorly known. The Essaouira Basin also contains four sub-basins: Ouazi basin, Iguerounzar basin, Ksob basin, and Igouzoullene basin.

Hydrologically, as shown in Figure 1, four main rivers cross the Essaouira basin: Ouazi Wadi in the northern part; Iguerounzar Wadi in the west, which drains the Cenomano-Turonian aquifer via several springs and originates from the High Atlas and crosses the Bouabout unit in a SE–NW direction; Ksob Wadi in the western part of the eastern basin originates from the confluence of the Iguerounzar and Zelten Wadis and constitutes a source of supply of the Plio-quaternary aquifer at the level of the Essaouira basin with a NW flow direction; Igouzoullene Wadi in the southern end, which drains the Hauterivian aquifer. The basin also contains two large dams: Zerrar, with a storage capacity of 70 Mm^3 (million cubic meters), and Igouzoullene, with a normal impoundment capacity of 17 Mm^3 [18]; these two impoundments respectively regulate the flows of the Iguerounzar and Igouzoullene Wadis.

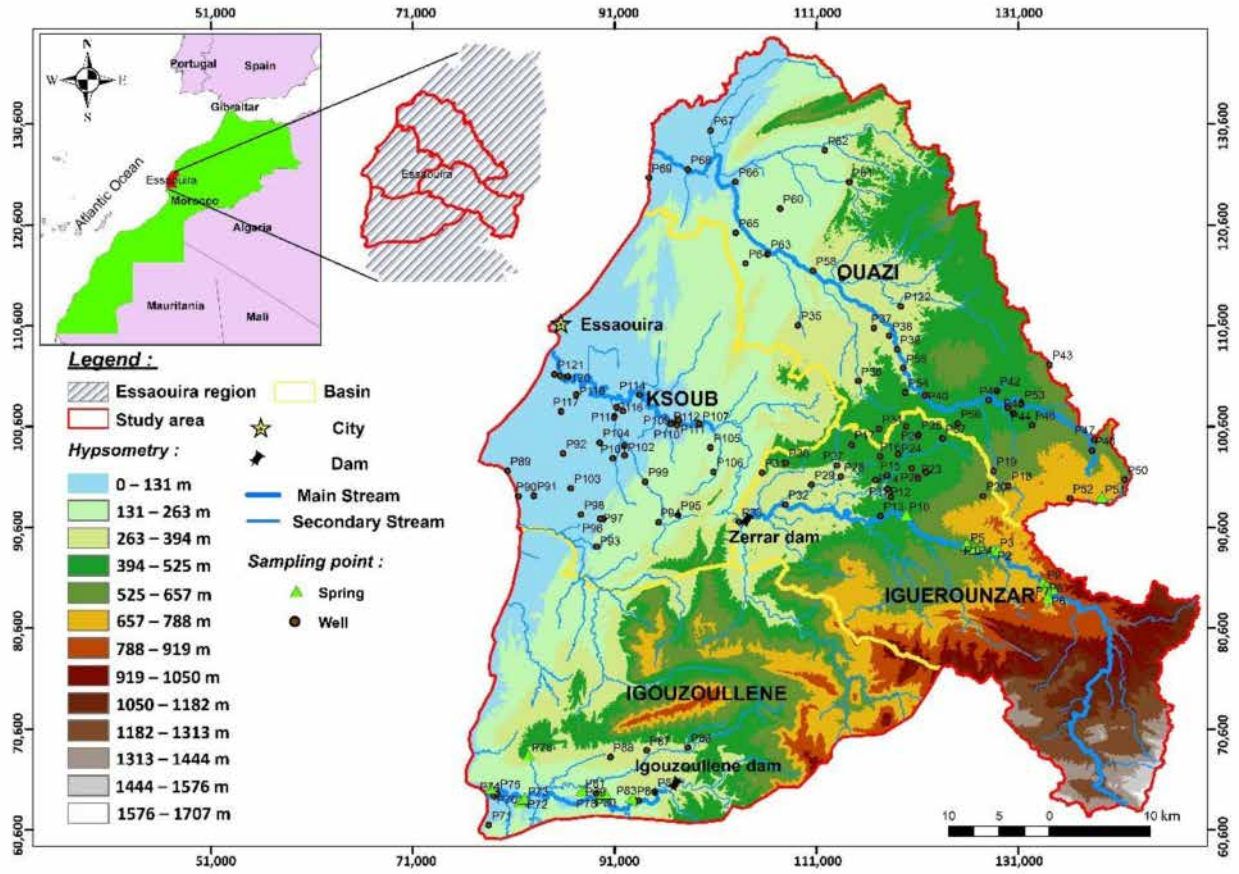

Figure 1. Geographic location of the study area and sampling points (Digital Elevation Model (DEM) source: https://glovis.usgs.gov/app).

Geological studies are imperative for understanding and explaining the chemistry of the waters within the basin. The geological formations constitute the host of these resources and are considered the first factors affecting their composition and the major cause of the mineralization.

The study area is characterized by a diversity of outcrops, ranging from the Lower Cretaceous to the Plio-Quaternary. Triassic and Jurassic formations take the form of reduced outcrops in the heart of the Tidzi, Amsitene, and Hadid anticlines, while the Tertiary and Quaternary formations are outcrops at the level of the synclinal basins (Figure 2 [19]). The Triassic formations consist of saliferous red clays, sandstone pelites, and dolerite basalts. The alternation of carbonate deposits (limestone and dolomite) and marls rich in evaporites (gypsum and anhydrite) correspond to Jurassic formations. Cretaceous and Quaternary formations, as shown in the stratigraphic log (Figure 3) that was redrawn and translated from [20]. The Lower Cretaceous formation is made up of limestone and marl alternating with some sandstone levels, with an average thickness of 200 m. The Middle Cretaceous formation begins with marl-sandstone deposits of the Aptian, followed by pyrite-green marls of the Albian, which are respectively 60 and 100 m thick. The Cenomanian formation is dominated by marly formations that are rich in anhydrites and interspersed with pastures of a few limestone levels with a thickness of 200 m.

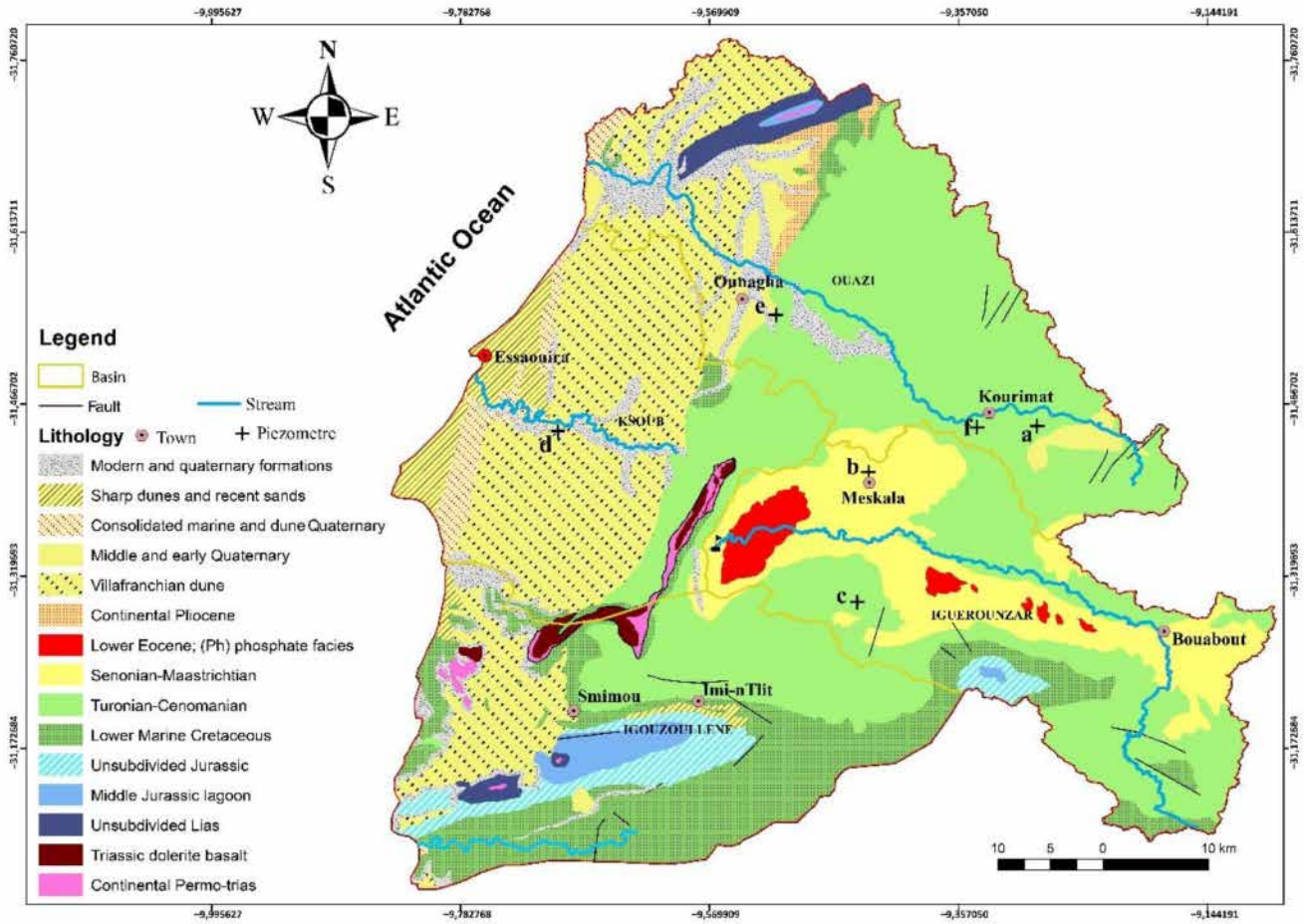

Figure 2. Geological map and location of the piezometric monitoring points (modified from [19]).

This last formation constitutes the wall of the 60-m-thick Turonian Calcaro dolomitic flint aquifer. The Cretaceous formation ends in dolomitic marls and limestones surmounted by gypsum and siliceous grey marls with Senonian sandstone pasture separating the Plio-Quaternary aquifer from the Turonian aquifer within the Essaouira basin [7,20]. The Essaouira basin is a vast synclinal zone that is affected by tectonics and diapirism, which gave rise to the numerous synclinal basins, such as the Essaouira basin downstream (crossed by the Ksob Wadi) and the Bouabout basin upstream (crossed by the Iguerounzar Wadi), where the two are separated by the saliferous diapir of Tidzi. Upstream, the Cenomano-Turonian aquifer was formed from limestones and dolomitic limestones and is limited at the base by lower Cenomanian grey clays and at the top by Senonian white marls [14]. Downstream, there are two main reservoirs, namely, the Plio-Quaternary and the Turonian. The first one has a matrix of marine calcareous sandstone, has a primary hydraulic conductivity by porosity, and contains a free water table. The second one contains an aquifer that is very quickly captive under the Senonian marl formations. The contacts between these aquifers are on the edges of the basin to the north toward the Ksob Wadi and to the west and east at the level of the hidden diapir of Essaouira and Tidzi, respectively [21,22].

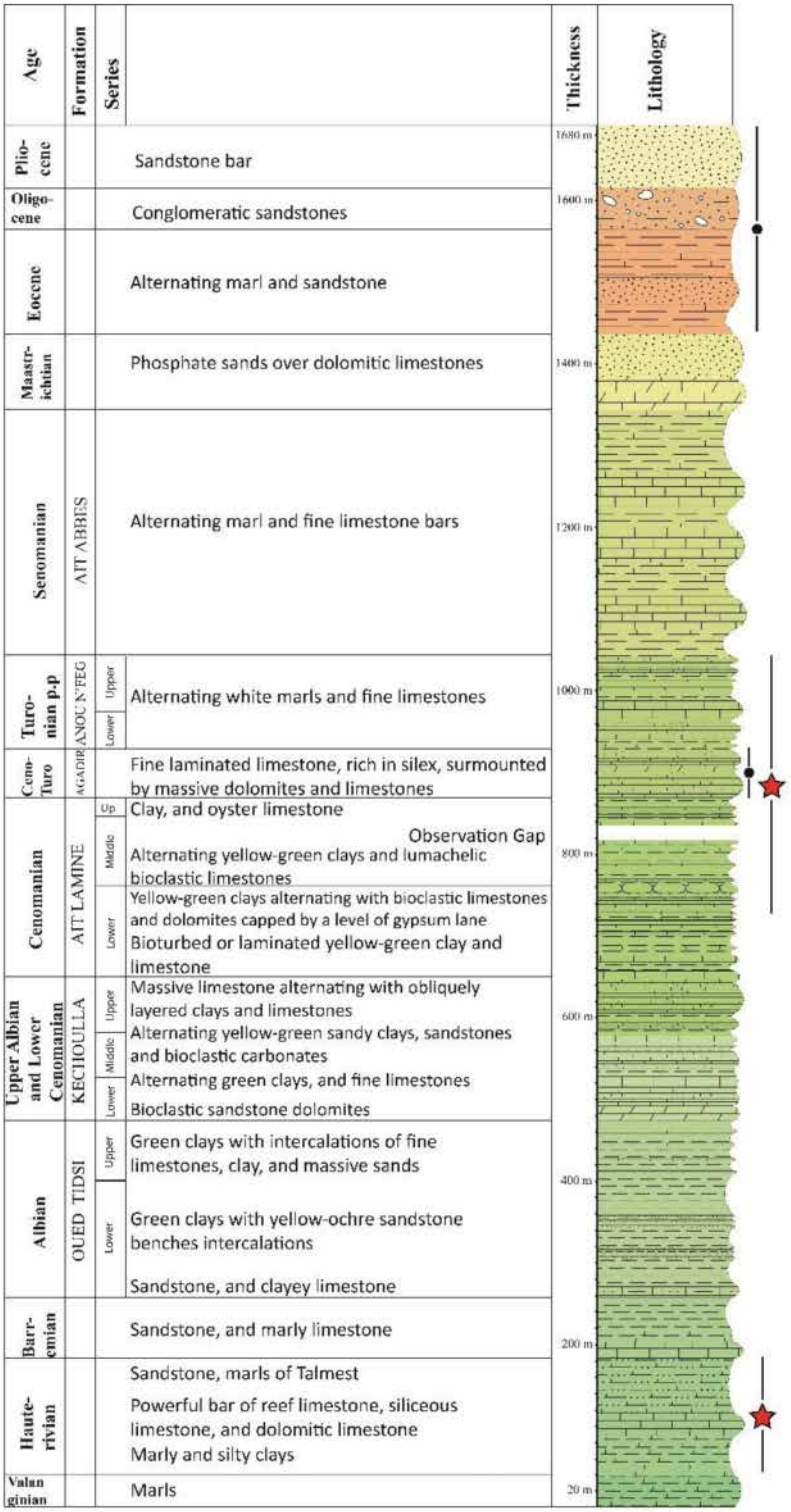

Figure 3. Lithostratigraphic log and aquifers in the study area (modified from [20]).

3. Materials and Methods

Water samples were collected in July 2020 from the four sub-basins of Essaouira: Ksob, Ouazi, Igouzoullene, and Iguerounzar. A total of 122 points were sampled (102 dug wells, 16 springers, and 4 boreholes) that captured the four aquifers, namely, Plio-Quaternary, Turonian, Cenomano-Turonian, and Hauterivian.

The usual physical parameters (pH, temperature, electrical conductivity, and total dissolved solids) were measured in the field using a portable Hanna HI-9828 conductivity

meter (HANNA Instruments, Lingolsheim, France). The water level was measured using a sonic piezometric probe (HANNA Instruments, Lingolsheim, France) with a range of 200 m.

The chemical analyses were performed using a SKALAR San++ Continuous Flow Analyzer (CFA) (SKALAR, Breda, Netherlands) for Ca^{2+}, Mg^{2+}, Cl^{-}, $SO_4{}^{2-}$, $NO_3{}^{-}$, and $HCO_3{}^{-}$. The Na^{+} and K^{+} contents were measured using atomic absorption spectrophotometry (AAS) at the Water, Soil, and Plant Analysis Laboratory of the Experimental Farm at Mohammed VI Polytechnic University of Benguerir in Morocco. The obtained results are grouped in Table 1.

Table 1. Statistical results of the analyzed samples (campaign of 2020).

Parameter	T	pH	EC	Ca^{2+}	Mg^{2+}	Na^{+}	K^{+}	Cl^{-}	$HCO_3{}^{-}$	$SO_4{}^{2-}$	$NO_3{}^{-}$
	(°C)		(µS/cm)	(mg/L)							
Cenomano-Turonian aquifer (n = 70)											
Maximum	26.7	8.2	5500	699.1	285.0	614.3	214.6	1569.0	680.0	2106.0	940.5
Minimum	19.6	7.0	640	68.7	14.7	22.0	0.6	40.4	161.0	26.0	0.1
Average	22.2	7.5	2370	196.8	94.9	161.1	10.5	442.0	358.6	272.5	57.4
SD	1.1	0.2	1097	90.5	45.6	106.7	9.8	319.2	64.7	193.6	43.7
Hauterivian aquifer (n = 18)											
Maximum	32.1	8.5	26,770	341.1	817.5	7117.6	231.0	11,574.5	510.0	2320.0	226.8
Minimum	22.1	6.6	481	18.6	8.2	39.2	2.5	45.0	141.5	90.8	0.2
Average	25.3	7.7	3116	126.3	99.8	542.5	18.6	928.8	362.3	289.6	20.7
SD	1.8	0.4	2737	41.1	79.7	746.1	24.2	1199.7	106.3	225.6	26.5
Plio-Quaternary aquifer (n = 26)											
Maximum	32.1	8.4	23,850	454.7	715.9	6079.3	214.3	10,741.2	470.9	2098.0	149.7
Minimum	20.5	6.5	775	51.6	12.9	70.9	1.8	80.7	144.0	23.5	1.9
Average	23.6	7.6	3022	154.0	82.2	462.3	17.0	887.3	304.3	221.9	42.5
SD	1.7	0.2	1904	58.5	55.4	437.3	18.4	846.3	63.4	147.4	36.4
Turonian aquifer (n = 6)											
Maximum	28.3	7.7	2606	198.4	80.1	270.3	12.4	639.3	366.0	256.4	60.5
Minimum	25.0	7.1	817	72.9	32.6	31.9	3.2	74.4	185.4	120.0	0.2
Average	26.7	7.5	2042	142.3	62.8	187.8	6.1	430.5	296.1	178.7	31.1
SD	1.1	0.2	491	42.0	11.9	59.4	2.3	139.3	64.8	37.3	23.1

EC: electrical conductivity, SD: standard deviation.

The interpolation algorithm used in this work was spatial prediction via linear kriging, which allowed for predicting the values of the EC at an unsampled site using a linear combination of adjacent point data.

For the monitoring of surface waters over 14 years, a GIS (geographic information system, was used in the processing of satellite images from LandSat 4–5 TM (Thematic Mapper, https://glovis.usgs.gov/app) and LandSat 8 OLI (Operational Land Imager, https://glovis.usgs.gov/app) sensors. The acquisition of satellite images requires a number of conditions to be taken into consideration, such as the availability of the image on the NASA website (www.glovis.usgs.org) and the presence of dust and clouds in the atmosphere, which sometimes makes viewing and interpreting the image difficult. Prior to the image processing phase, radiometric and atmospheric corrections were made using ENVI 5.3 software (L3Harris Geospatial, Boulder, CO, USA). The detection of water was done using the calculation of the NDWI (normalized difference water index), which uses the near-infrared band and a shortwave infrared (SWIR) band [23] between 1500 and 1750 nm, where water has an absorption peak. The near-infrared (NIR) band was used because water does not absorb in this region of the electromagnetic spectrum. The NDWI can be calculated in such a way as to focus just on water surfaces without confusion with plant and soil moisture; this allows for the estimation of the evolution of water surfaces by comparing a series of satellite images from different periods. The NDWI is calculated according to the following Equation (1):

$$NDWI = (NIR - SWIR)/(NIR + SWIR). \quad (1)$$

The data from the 2017, 2018, and 2019 campaigns that were carried out during low water periods for the same water points [17,24,25] were also used to monitor changes in the physical parameters of the water under climate change forcing.

The Mann–Kendall test [26,27] was used to examine the existing linear trend in this rainfall time series. This test defines the U_{MK} standard (multi-variable standard) as the x_i series (x_1, x_2, ..., x_n), as follows (Equation (2)):

$$U_{MK} = \frac{S}{\sqrt{\mathrm{Var}(S)}}, \quad S = \sum_{i=1}^{n-1} \sum_{j=i+1}^{n} \mathrm{sgn}(x_j - x_i), \mathrm{Var}(S) = \frac{n(n-1)(2n+5)}{18}, \tag{2}$$

where n is the number of data in the series.

The Mann–Kendall statistical coefficient U_{MK} defines the direction of the trend. If U_{MK} is positive, the trend is upward; if U_{MK} is negative, then the trend is downward.

4. Results and Discussion

4.1. Precipitation

The rainfall data used in this study were obtained from the Tensift Hydraulic Basin Agency (ABHT, Marrakesh, Morocco). The analysis of the annual precipitation data for a period of 38 years (1978–2015) for the investigation area revealed significant variability (Figure 4a).

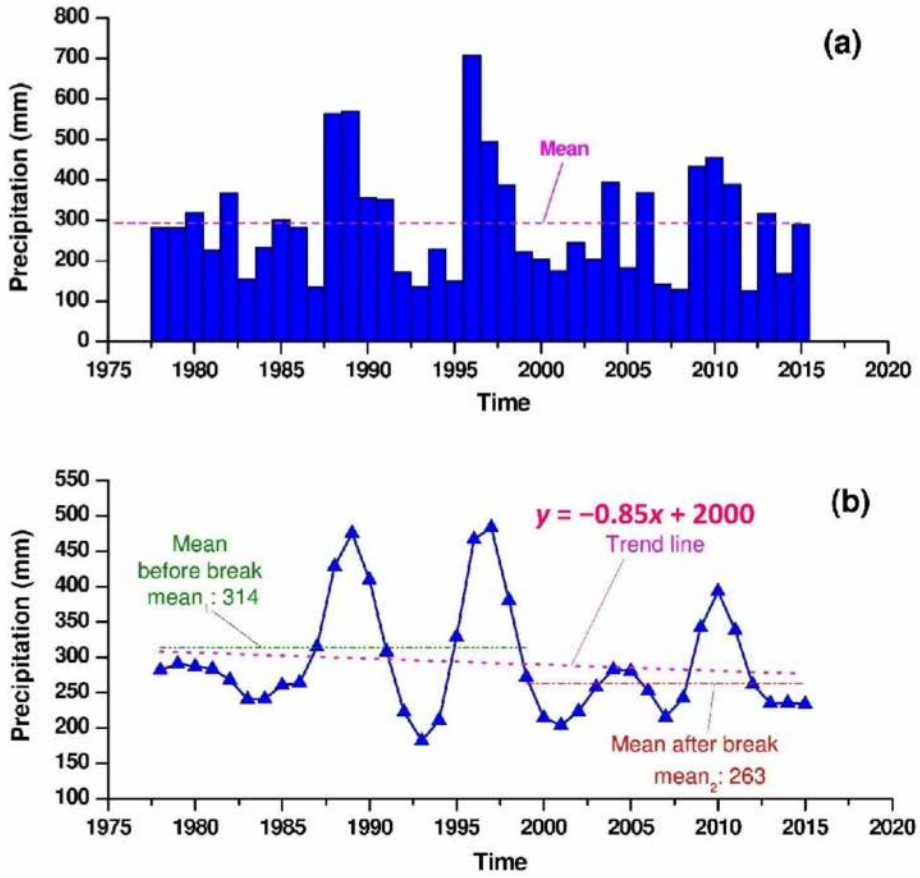

Figure 4. (**a**) Annual precipitations and (**b**) Pettitt test results.

Table 2. The results of the Mann–Kendall test.

Station	*p*-Value	Alpha	U_{MK}	Trend
Iguerounzar	0.009	0.05	−1.1	Decline

This parameter is subject to fluctuations from one year to another. Precipitation values varied between a minimum of 135 mm (in 2008) and a maximum of 707 mm (in 1996), with an average of 300 mm. The application of the Pettitt test (Figure 4b) with alpha equal to 0.05 showed the presence of a break in the rainfall series in 1998. The annual rainfall means before and after this break were 314 and 263 mm, respectively. This led to an estimated deficit rate of 16.24%. The Mann–Kendall test results (Table 2) showed a negative multivariable standard normal ($U_{MK} = -1.1$), reflecting a downward trend in rainfall that confirmed the results of the Pettitt test.

The monthly variations (Figures 5 and 6) showed a decrease in rainfall from one year to the next, which seemed to be the result of climate change, with June, July, and August representing the deficit months for the whole series, with maximums of 6 mm, 2 mm, and 8 mm, respectively. The wet months (extreme values), namely, November and December, displayed maximum values of almost 200 mm.

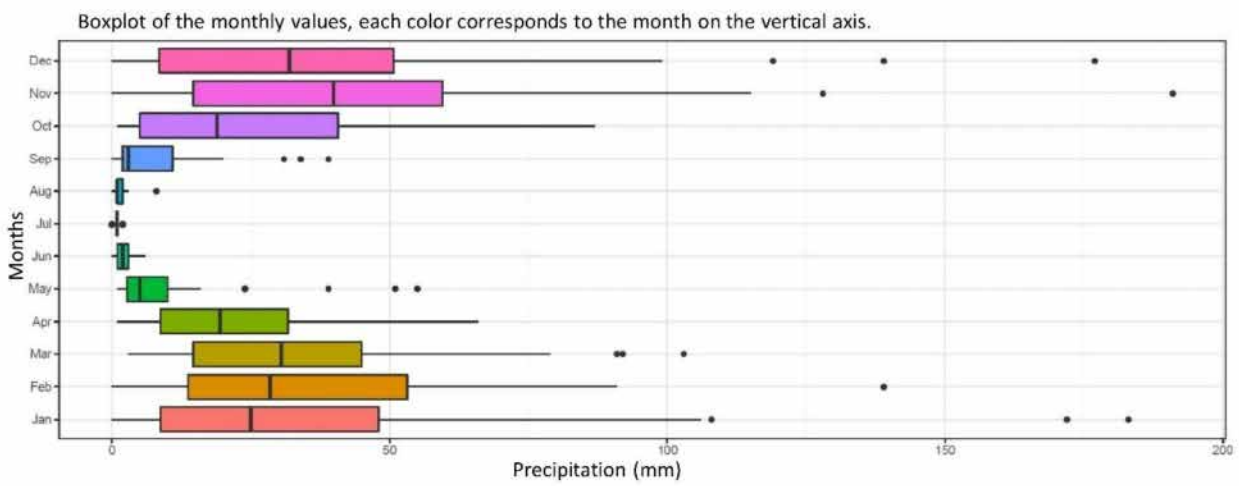

Figure 5. Boxplot of monthly values between 1979 and 2019.

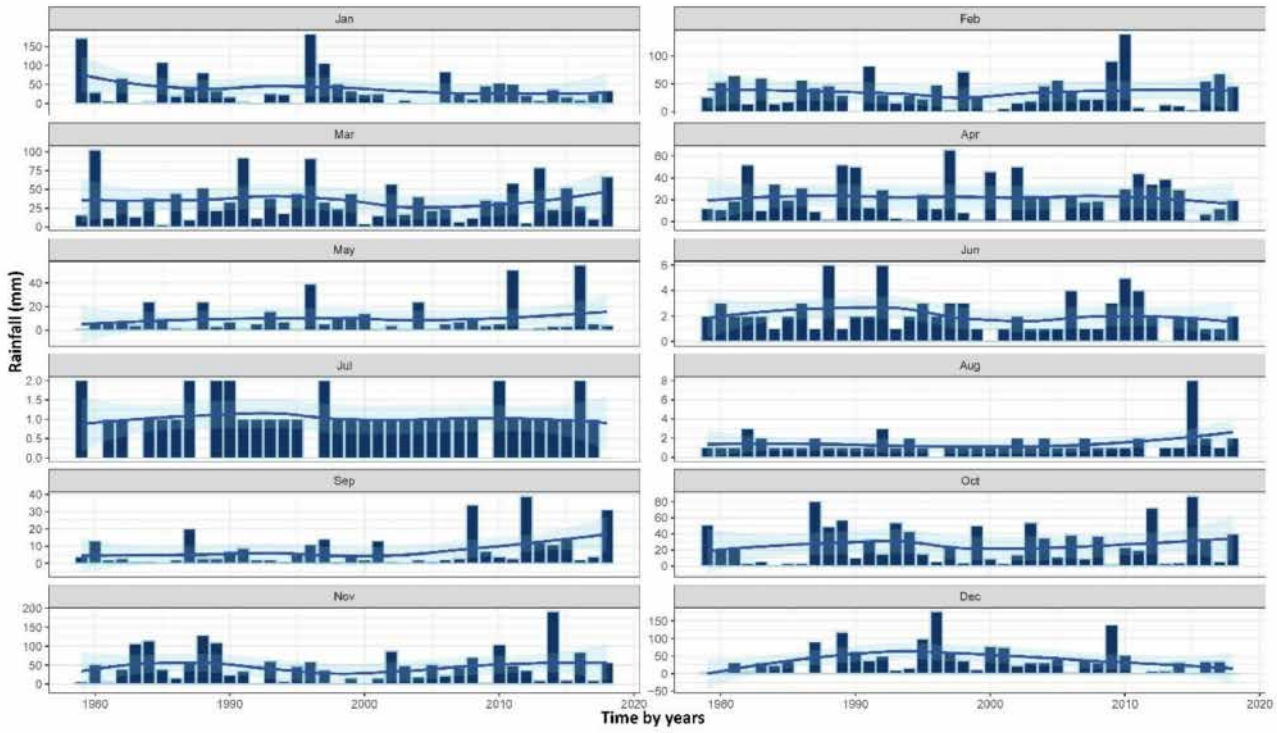

Figure 6. Monthly variation in rainfall (mm) between 1979 and 2019.

4.2. Piezometry

The variation in piezometric levels is controlled by several factors, such as the decrease in rainfall as a result of climate changes and the overexploitation of water resources. In this study, three aquifers were monitored piezometrically, namely, the Plio-Quaternary, Cenomano-Turonian, and Hauterivian aquifers (Figure 7).

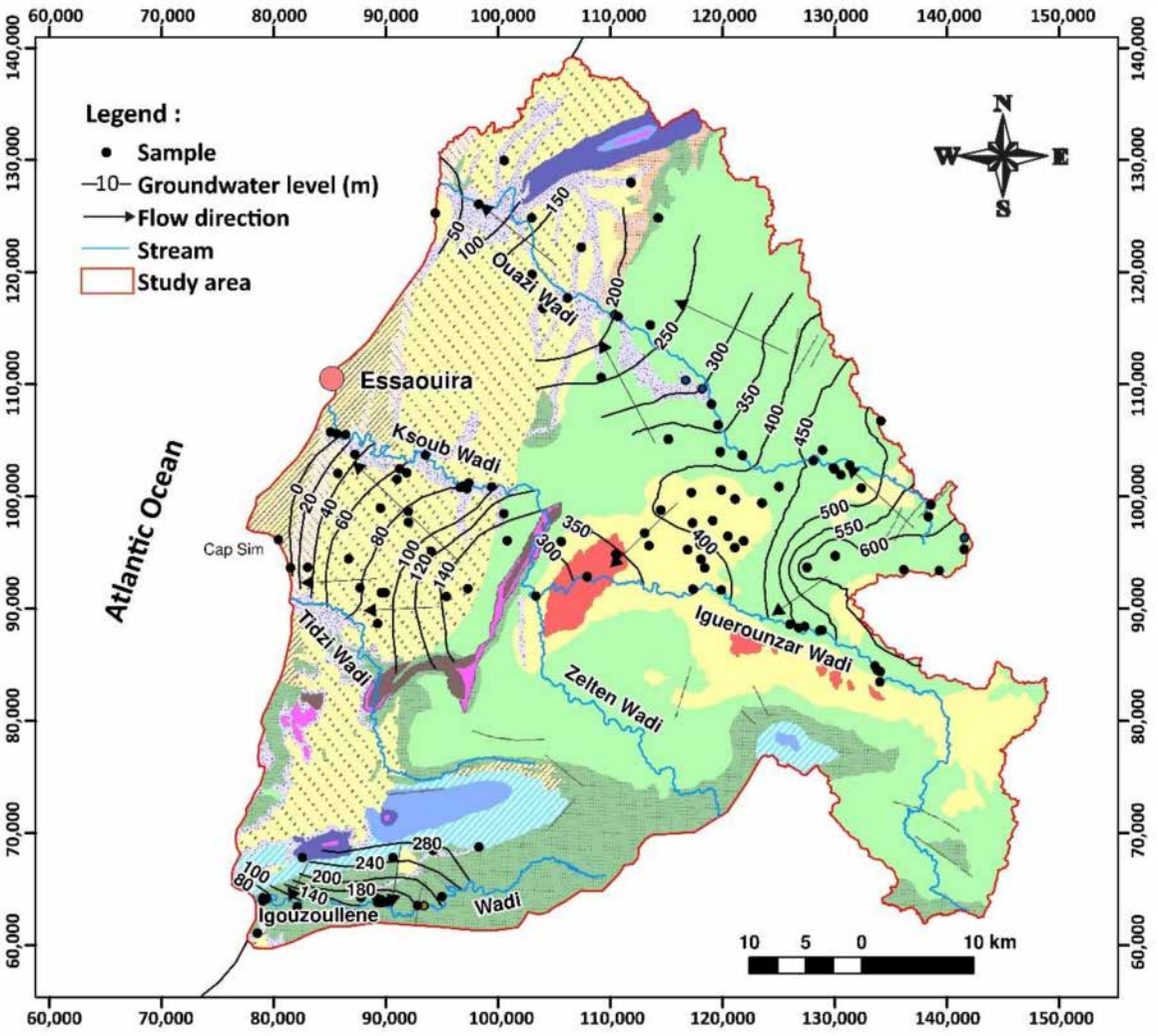

Figure 7. Piezometric map of the study area (campaign of 2020).

The piezometric map of the Plio-Quaternary aquifer shows a flow from SE to NW in the northern part and from NE to SW in the downstream part. This direction was conditioned by the substratum of the aquifer and by the hidden diapir of Essaouira. The hydraulic gradient was equal to 1.5% in the upstream part, 0.7% in the central part, and 1.2% in the downstream part.

The groundwater of the Cenomano-Turonian aquifer presented a flow whose direction was from SE toward the NW in its northern part at the level of the Ouazi Wadi and from N toward the S in its southern part in the Meskala basin. The hydraulic gradient was 2.5% in the upstream part, 1.1% in the central part, and 1.6% in the downstream part. To the south, the Igueriounzar Wadi drained the entire Cenomano-Turonian aquifer through more than 14 springs. According to the survey and field observations, the Cenomano-Turonian aquifer provided ecological and socio-economic stability to the inhabitants and the plant and animal species that populate the rural communes along the Igueriounzar Wadi. The current overexploitation of this essential resource and the cyclicality of drought following climate change can only lead to water, environmental, economic, and social crises in the short term.

The dependence on this natural heritage is very strong and requires the mobilization of all means to conserve it.

The groundwater of the Hauterivian aquifer showed a flow from north to south. The Igouzoullene Wadi drained the entire aquifer with a north to south flow with a hydraulic gradient of 2.3% in the eastern part and 6% in the western part.

The monitoring network, with a monthly step (only one measurement per month) for a period of 10 years (2006–2016), of the four aquifers showed a decrease (Figure 8) in water level in the six piezometers (a, b, c, d, e, and f) monitored in the basin. This decrease was controlled by several factors, including the decrease in precipitation that was probably due to the effects of climate change [16]. The problems of water scarcity and cyclicality of droughts have been claimed in the Essaouira region in recent decades [9]. The piezometric contour lines for the six points have negative slopes, which mean a drop in water level.

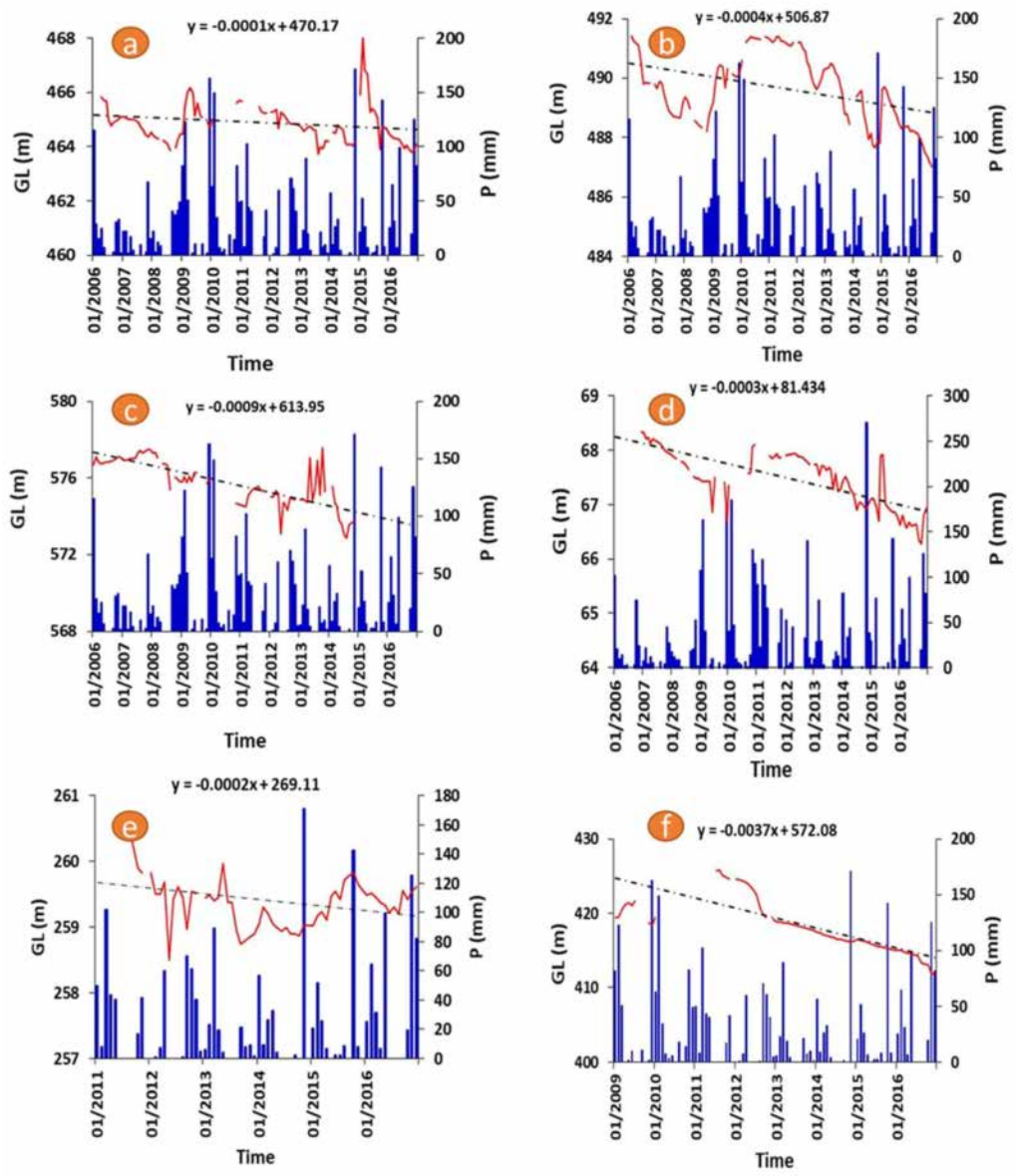

Figure 8. Groundwater levels' evolution between 2006 and 2016 ((**a**–**f**) are piezometric monitoring points for the locations, see Figure 2). GL: groundwater level, P: precipitation.

4.3. Physicochemical Characteristics

4.3.1. Electrical Conductivity (EC)

EC is a determining factor for the quality of water. It corresponds to the capacity of water to transmit electrical current between two metal electrodes with a surface area of 1 cm^2 and separated from each other by 1 cm [28]. It reflects the degree of mineralization of the water and is expressed in Siemens per centimeter (S/cm). In the Essaouira region, which opens onto the Atlantic Ocean, conductivity measurements are of great importance for explaining either the degree of dissolution of the surrounding rocks or the contamination degree of the groundwater by seawater. The EC values of groundwater of the Plio-Quaternary, Turonian, Hauterivian, and Cenomano-Turonian aquifers recorded in 2017, 2018, 2019, and 2020 showed an increasing trend in time and space (Figures 9–11).

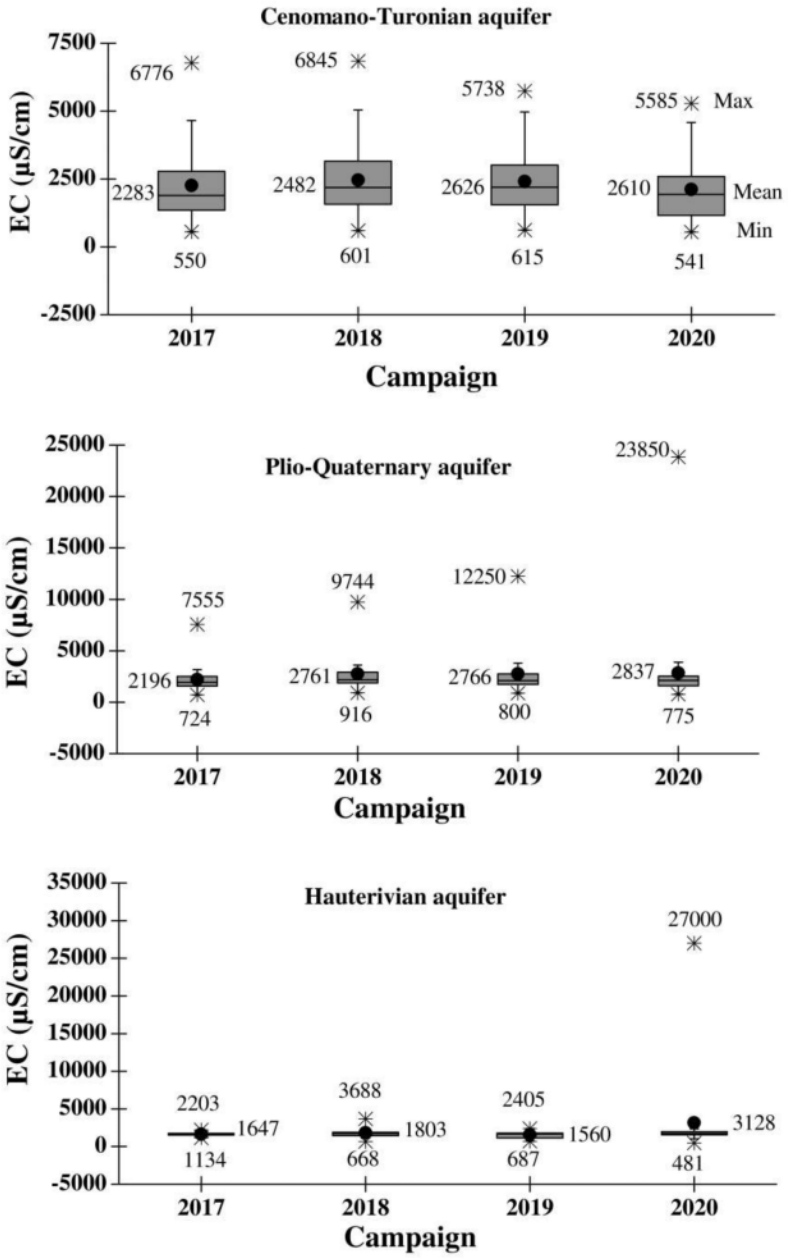

Figure 9. Electrical conductivity statistics for the 2017, 2018, 2019, and 2020 campaigns for the Cenomano-Turonian, Plio-Quaternary, and Hauterivien aquifers.

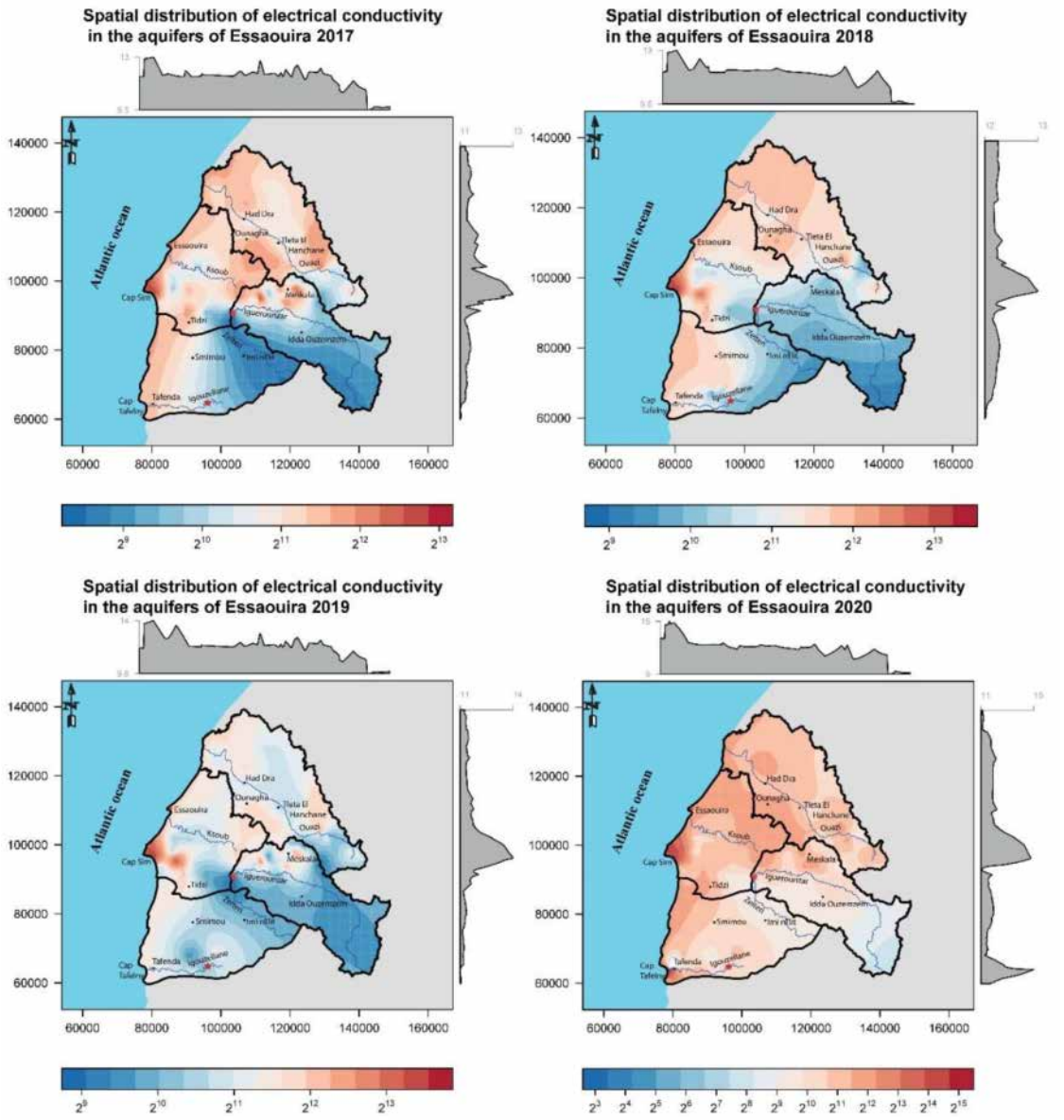

Figure 10. Spatial distribution of electrical conductivity in Essaouira's aquifers between 2017 and 2020.

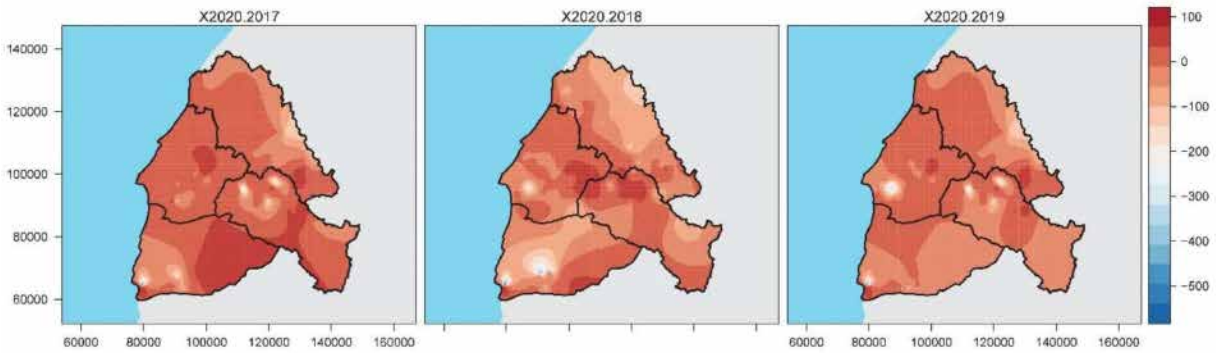

Figure 11. Comparison of the state of the EC in 2020 compared to the years 2017, 2018, and 2019.

The maps in Figure 10 correspond to the presentation of the EC status in the study area for the sample campaigns from 2017 to 2020. In 2017, the EC varied between 550 and 7555 µS/cm, with an average of 2185 µS/cm; there was a decrease in the EC when moving away from the edge of the Atlantic Ocean. According to the quality standards,

based on conductivity values, more than 79% of the points sampled in this year were of average-to-poor quality. The sampling points that were most affected by the strong mineralization were around Meskala, Ounagha, Tidzi, Cap Sim, and the northern end of the Ouazi Basin.

For the campaign of 2018, the EC values varied between 668 and 9744 µS/cm, with an average of 2399 µS/cm. The EC values generally increased homogeneously throughout the study basin; this is visible in the curves on the right and top of the maps, which represent the maximum values in the rows and columns, respectively. A total of 81% of the water points were average-to-poor quality.

Concerning the campaign of 2019, the EC values varied between 550 and 12,250 µS/cm, with an average of 2340 µS/cm. According to the monitoring carried out in the work of [19,25], the values of conductivity oscillated between 1990 and 2017, but never exceeded 8000 µS/cm, which are values that can be represented by a linear interpolation method of the variable in relation to the small values recorded. The year 2019 was characterized by the appearance of extreme values, which made it necessary to use a logarithmic scale with base 2. The quality of 82% of the sampled points was classified as average-to-poor. The majority of these points were located around Meskala (Cenomano-Turonian aquifer), south of the Ksob Wadi in the Essaouira basin (Plio-Quaternary and Turonian aquifers), north of the Ouazi basin, and the west end of the Igouzoullen basin (Hauterivian aquifer).

For the campaign of 2020, the EC values varied between 481 and 27,000 µS/cm, with an average of 2469 µS/cm. The spatial distribution and the curves of the extreme values of the EC displayed several zones with anomalies that produced an increase in the salinity of the waters. Cap Tafelny and Cap Sim were the most affected due to the impact of brackish water from the sea.

The EC, which reflects the water's mineralization degree, which destroys the quality of this natural wealth, is mainly due to the decrease in rainfall as a result of climate change, overexploitation, dissolution of the casing, marine intrusion, and polluting discharges. The results of the EC presented lead to the claim that the most intervening factor in the groundwater mineralization in the Essaouira region was the marine intrusion, coupled with climate change; this was confirmed by the observed electrical gradient, which decreased from the coastal edge to the mainland. The Zerrar dam (commissioned in 2008), which is located at the intersection of the Iguerounzar and Zelten Wadis, as well as the Igouzoullene dam (commissioned in 2004), probably had an effect on the regulation of the groundwater salinity through the infiltration of water from the reservoirs via porosity (dilution effect). The monitoring of the spatiotemporal evolution of electrical conductivity (Figure 11) showed an increase in these values from 2017 to 2020. The high values recorded showed the critical state of water resources in the Essaouira basin. The comparison between the values observed in 2017, 2018, and 2019 with those of 2020 showed a remarkable increase in groundwater mineralization. This increase was 100% in some places, especially in the north of the Ouazi basin and in the Cap Sim.

4.3.2. Hydrogen Potential (pH)

The pH is the concentration of H^+ ions in the water, where the determination of this value is of great importance because it controls several physicochemical balances. It depends primarily on the origin of the water, the nature of the surrounding environment (geology), human activity, the degree of contamination by pollutants, and the climatic conditions (precipitation and temperature). Natural waters often have a pH value between 6 and 8.5. In our study area, where most of the geological formations are made up of limestone, the pH varied from 7.1 to 8.3, and therefore constituted a biotope that was favorable for the development of life.

For the study area, the values recorded in the four aquifers varied from 6.5 to 8.5, with an average of 7.51 (Figure 12), which confirmed that the waters in this basin met the standards set by [29].

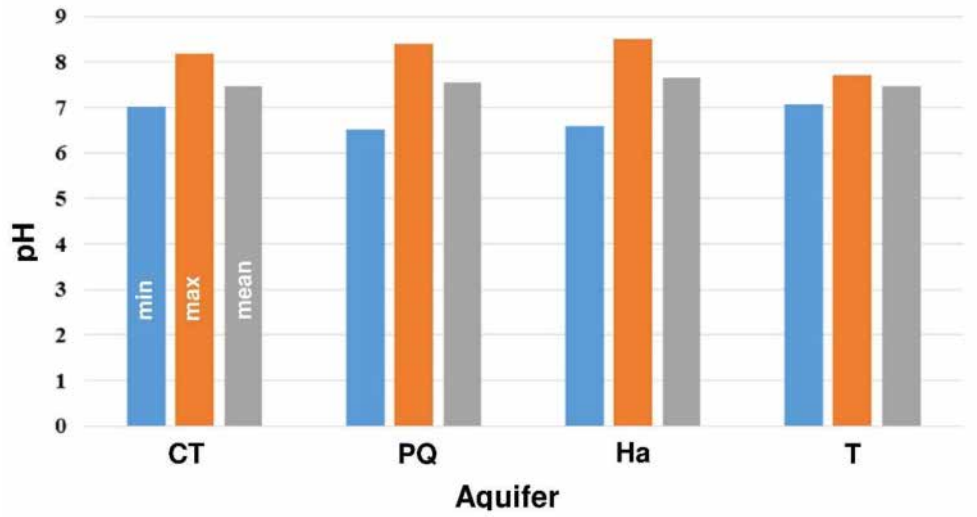

Figure 12. pH variation in the aquifers (2020 campaign). CT stands for Cenomano-Turonian, PQ stands for Plio-Quaternary, Ha stands for Hauterivian, and T stands for Turonian.

4.3.3. Chemical Facies

The increasing demand for water has caused enormous pressures on the water resource, which has resulted in the degradation of its quality in the study area. This degradation has become more serious in recent years under the effect of climate change.

The projection of major element concentrations (cations and anions) on the Piper diagram ([30], Figure 13) showed that the groundwater of the four aquifers, namely, Cenomano-Turonian, Plio-Quaternary, Hauterivian, and Turonian, had the facies: Cl-Ca-Mg, Cl-Na, HCO_3-Ca-Mg, SO_4-Ca, and HCO_3-Na, with the dominance of the Cl-Ca-Mg type. Point P92 capturing the Plio-Quaternary aquifer, located in the south of the Ksoub Wadi, presented HCO_3-Na facies. Points P48 and P58, which captured the Cenomano-Turonian aquifer near the Kourimat village, presented SO_4-Ca facies.

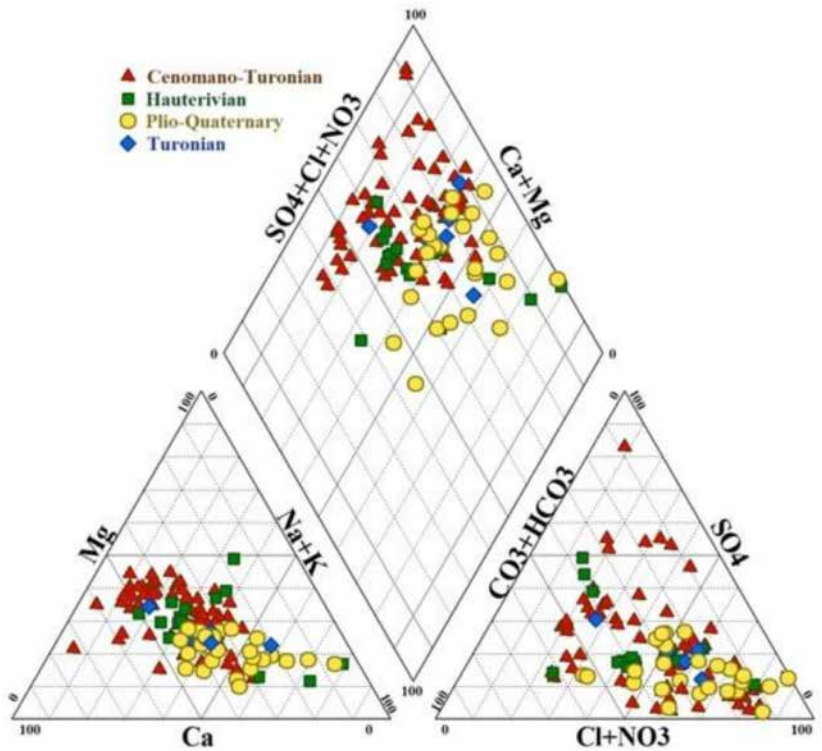

Figure 13. Piper diagram of the analyzed samples (campaign of 2020).

4.3.4. Origin of the Groundwater Mineralization

To understand the processes that contribute to the groundwater mineralization in the Essaouira basin, major element correlation diagrams have been established (Figure 14).

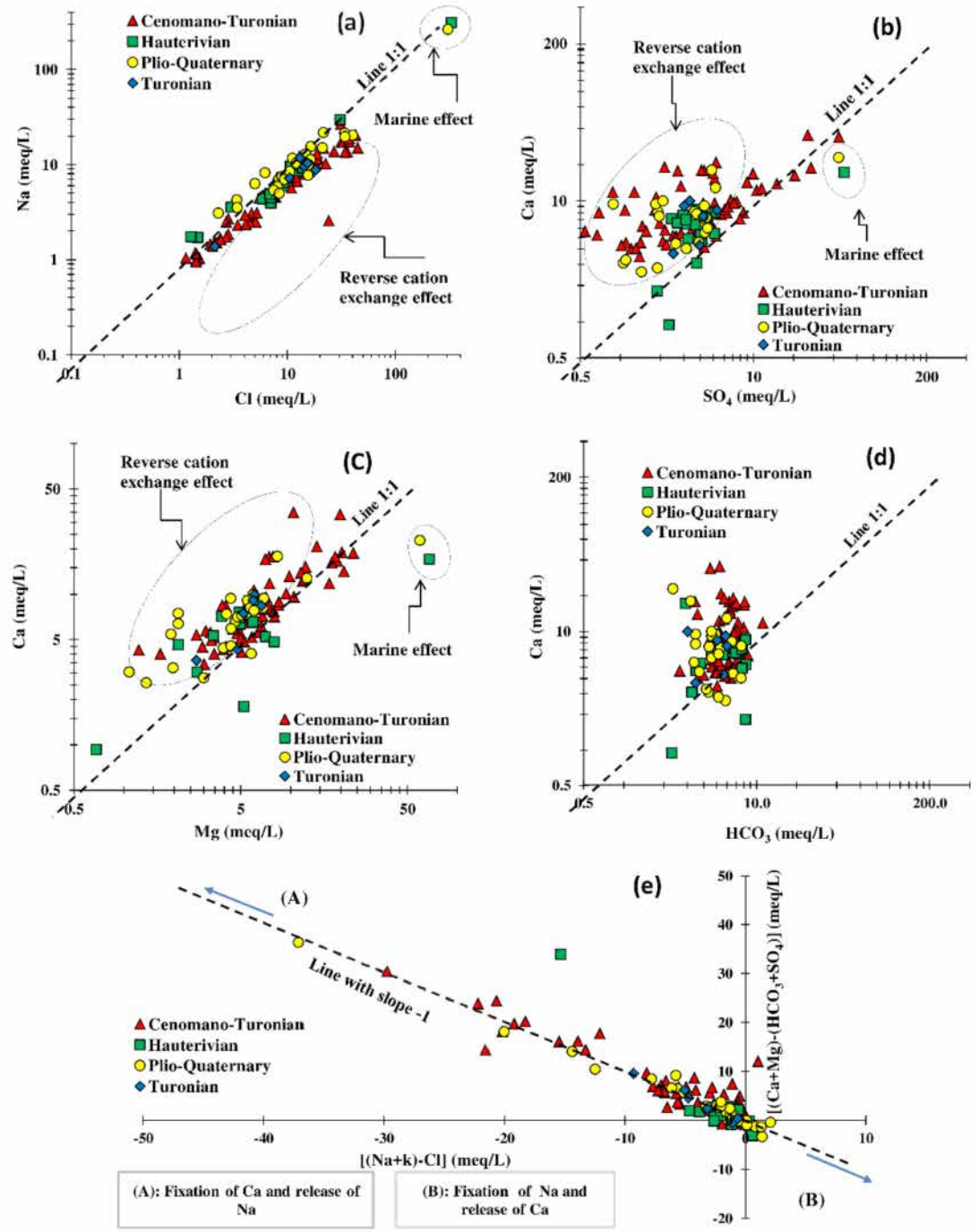

Figure 14. Correlation diagrams: (**a**) Na^+ vs. Cl^-, (**b**) Ca^{2+} vs. $SO_4{}^{2-}$, (**c**) Ca^{2+} vs. Mg^{2+}, (**d**) Ca^{2+} vs. $HCO_3{}^-$, and (**e**) $Ca^{2+} + Mg^{2+} - HCO_3 - SO_4{}^{2-}$ vs. $Na^+ + K^+ + Cl^-$ (campaign of 2020).

Figure 14a shows a strong positive correlation between Na^+ and Cl^-. This indicates that these two elements had the same origin. Some points were aligned with the 1:1 line, reflecting the contribution of the dissolution of halite, which is an orange or red saliferous clay, to groundwater mineralization. This hypothesis was confirmed by negative saturation indices with respect to halite (Figure 15a). The rest of the samples were located below the 1:1 line, reflecting a deficit in Na^+ compared to Cl^-. This deficit was explained by the

contribution of the reverse cation exchange phenomenon to the groundwater mineralization in the study area by the release of Ca^{2+} and the fixation of Na^{+} by the aquifer matrix (Figure 14e). The two points P74 and P89 had Ca^{2+} and Cl^{-} contents that were greater than 100 meq/L, which suggests contamination by seawater in accordance with their location close to the ocean.

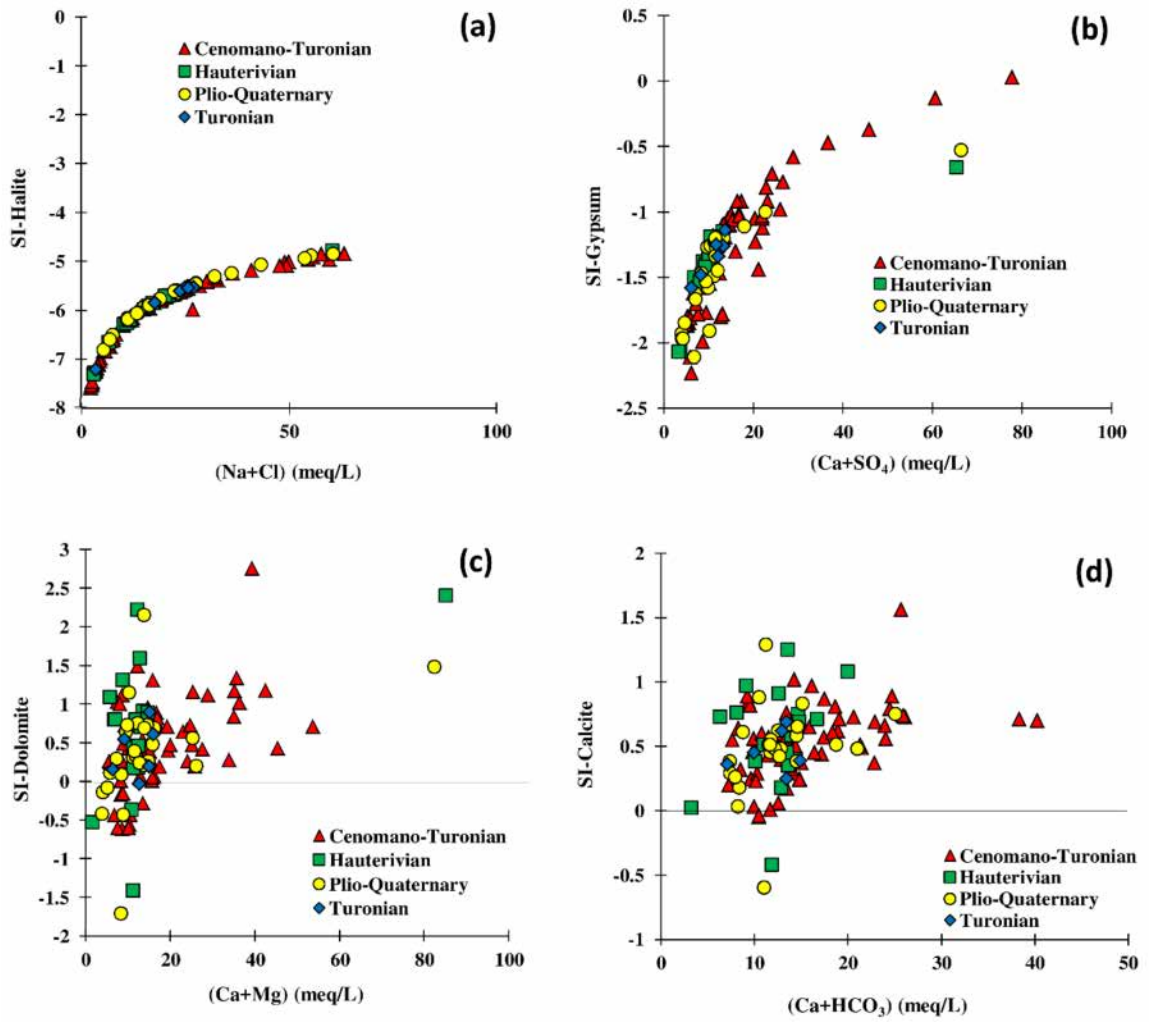

Figure 15. Correlation diagrams: (**a**) SI-halite vs. $Na^{+} + Cl^{-}$, (**b**) SI-gypsum vs. $Ca^{2+} + SO_4{}^{2-}$, (**c**) SI-dolomite vs. $Ca^{2+} + Mg^{2+}$, and (**d**) SI-calcite vs. $Ca^{2+} + HCO_3{}^{-}$. SI: Saturation index, (campaign of 2020).

The correlation between Ca^{2+} vs. $SO_4{}^{2-}$ (Figure 14b) showed that some points were scattered around the gypsum dissolution line (line 1:1). This suggested the contribution of gypsum dissolution in the mineralization of the waters of the study area. This hypothesis was corroborated by negative saturations index values with respect to the gypsum (Figure 15b). The rest of the points were located above the 1:1 line, reflecting an excess of Ca^{2+} over $SO_4{}^{2-}$. This suggested the contribution of the reverse cation exchange phenomenon to the groundwater mineralization of the four aquifers studied (Figure 14e).

The Ca^{2+} vs. Mg^{2+} correlation diagram (Figure 14c) shows that some samples were scattered around the dolomite dissolution line, reflecting the contribution of this mineral to the groundwater mineralization in the study area. This was supported by negative saturation index values with respect to dolomite (Figure 15c). Some points showed positive saturation indices with respect to dolomite, reflecting the saturation of the waters at these points in dolomite. The rest of the points were located above the 1:1 line, reflecting an excess of Ca^{2+} over Mg^{2+}. This excess could be explained by the reverse ion exchange phenomenon (Figure 14e).

Regarding the saturation indices with respect to the calcite, except for the two points P74 and P89, all the points had positive values (Figure 15d), reflecting the saturation of the water in the study area with respect to the calcite. This claim of saturation was supported by the low correlation between the Ca^{2+} and HCO_3^- contents (Figure 14).

4.3.5. Groundwater Quality for Drinking Purposes

Assessment of the groundwater quality for drinking purposes was carried out by comparing the chemical parameters of the analyzed samples with the thresholds set by [29]. The results obtained were grouped in Figure 16. Based on the Cl^- contents, all the groundwater in the four aquifers had levels above the threshold set by the World Health Organization (WHO). With the exception of the waters of the Plio-Quaternary aquifer, the waters of the other aquifers had Na contents below the threshold set by the WHO. Based on the contents of Ca^{2+}, Mg^{2+}, HCO_3^-, and NO_3^-, all waters showed concentrations lower than those accepted by the WHO. Concerning the SO_4^{2-} contents, the waters of the two aquifers Cenomano-Turonian and Hauterivian had concentrations above the limits set by the WHO, while the Plio-Quaternary and Turonian aquifers had the reverse. However, the groundwater from the aquifers studied requires treatment before being consumed, in particular, for Cl^- and SO_4^{2-}.

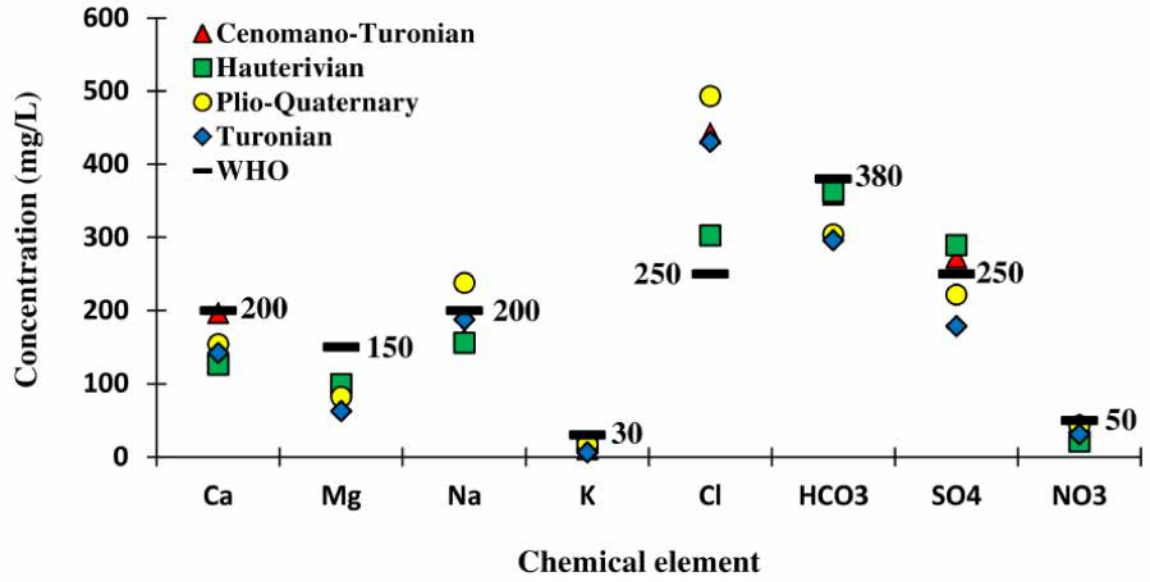

Figure 16. Comparison of chemical element contents (campaign of 2020) with the World Health Organization (WHO) standard values.

4.3.6. Groundwater Quality for Irrigation Purposes

The sodium percentage (Na%) [31] is one of the indices used to assess the suitability of groundwater for irrigation purposes. The Na% index has five classes: excellent, good, permissible, doubtful, and unsuitable. The values calculated in the study area varied between 4.4 and 51.5% for the Cenomano-Turonian aquifer, between 16.1 and 77.2% for the Hauterivian aquifer, between 31.1 and 75% for the Plio-Quaternary aquifer, and between 17.6 and 55.6% for the Turonian aquifer (Figure 17). According to the calculated values for the Cenomano-Turonian aquifer, 4% of samples were excellent, 40% were good, 26% were within doubtful limits, and 30% were unsuitable (Figure 17). For the Hauterivian aquifer, 5% of samples were excellent, 68% were good, 5% were within permissible, 11% were doubtful, and 11% were unsuitable (Figure 17). As for the Plio-Quaternary aquifer, 46% of the samples were excellent, 35% were doubtful, and 19% were unsuitable. Concerning the Turonian aquifer, 33% of the samples were of excellent quality, and 67% were of doubtful quality.

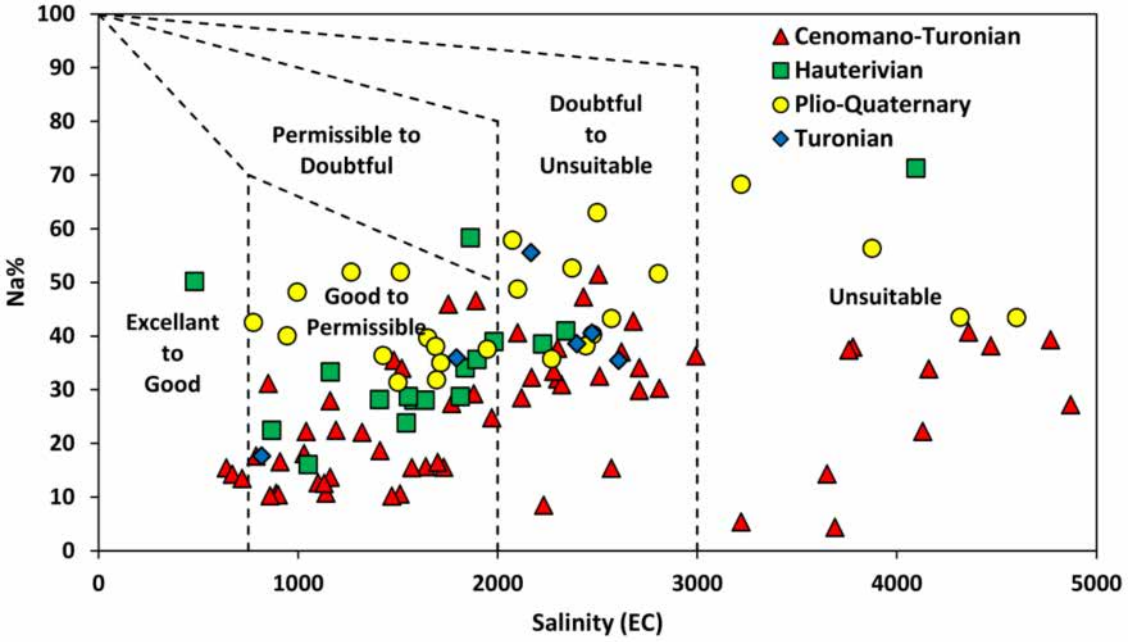

Figure 17. Wilcox diagram of the analyzed samples.

Sodium Adsorption Ratio (SAR) is an important parameter that is widely used to assess groundwater for irrigation purposes [32]. The SAR vs. salinity diagram (Figure 18) is a 16-compartment diagram, where each compartment corresponds to a SAR hazard and a salinity risk [32]. To get an idea about the suitability of the groundwater from the study area for agricultural purposes, the analyzed samples were projected onto the SAR vs. salinity diagram (Figure 18). The water points were projected onto the C2S1, C3S1, C4S1, and C4S2 compartments. The line S1 corresponds to a low risk of SAR, while the two columns C3 and C4 correspond to a high salinity and very high risk, respectively. Water with a SAR < 10 meq/L corresponds to adequate water for agricultural purposes [32,33]. With the exception of three samples from the Plio-Quaternary aquifer and one from the Hauterivian aquifer, the rest of the water points had SAR values below 10 meq/L. However, the groundwater of the studied aquifers was adequate for agricultural purposes, especially, for plants that adapt to high and very high salinity and low SAR risk.

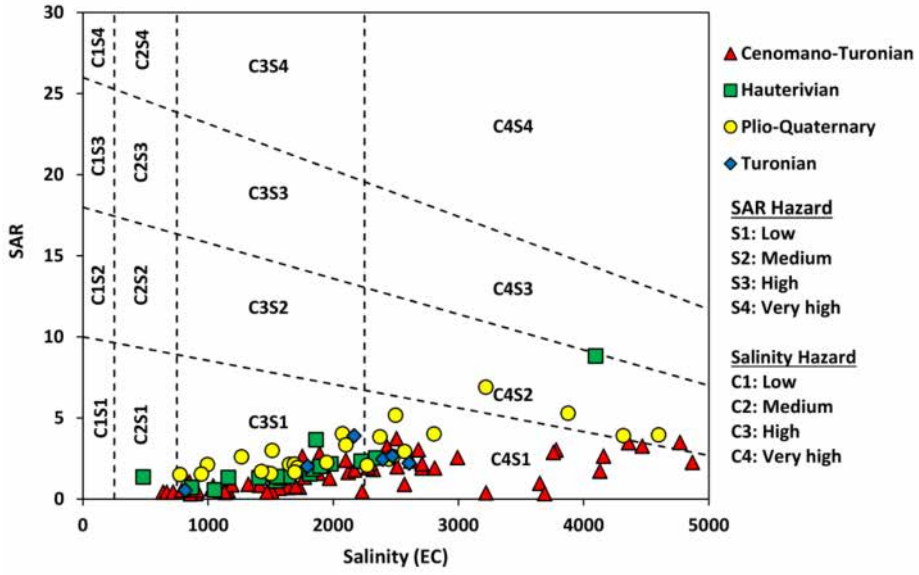

Figure 18. United States Salinity Laboratory (USSL) salinity hazard diagram of the analyzed samples.

4.4. Monitoring of the Surface Water Variations Using Remote Sensing (TM and OLI Sensors)

The Essaouira region belongs to one of the regions with a semi-arid climate. The geographical position of our study area and the global climate changes have imposed a very irregular rainfall pattern in time and space, which induces strong evapotranspiration. These climatic factors lead to a scarcity of surface water.

The NDWI calculated from the images from the TM and OLI sensors, which is calibrated and corrected for atmospheric effects, produces values between 1 and −1. The average value of water in the Essaouira region was approximately 0.24, as determined from the average reflectance of the water surface in the six images studied. From this value, it was possible to map the water surfaces in order to follow their dynamics in time and space.

Table 3 shows the variations in water surfaces in the basin. These surfaces were limited in the Igouzoullene and Zerrar dams, open water storage basins, such as the one for wastewater in the north of Essaouira, and in the estuaries of the wadis. Since the water surfaces were very limited and minimal in relation to the total surface area of the study basin, the water surfaces in the Essaouira region were very variable, as shown in the fluctuations in Table 3, with the largest being observed in 2016 and 2020. During the 14 year time span shown in Table 3, the surface occupied by water evolved by an estimated 6.24 km^2. This was due to the commissioning of two large dams. Between 2016 and 2020, there was an estimated 4.85 km^2 decrease in water surface area due to the decrease in rainfall.

Table 3. Synthetic table of the evolution of water surfaces between 2006 and 2020 in the region of Essaouira, as calculated using the normalized difference water index.

Date	Sensor	Area (km^2)	Area (%)	Exchange Rate
2006	LandSat 4–5 TM	1.069	0.025	
2010	LandSat 4–5 TM	8.097	0.188	0.163
2014	LandSat 8 OLI	7.880	0.183	−0.005
2016	LandSat 8 OLI	12.169	0.282	0.099
2017	LandSat 8 OLI	9.202	0.213	−0.069
2020	LandSat 8 OLI	7.311	0.170	−0.044

TM: Thematic Mapper, OLI: Operational Land Imager. (The green color: increase. red color: decrease).

5. Conclusions

For several decades, the protection and conservation of water quality have become a major concern and a main objective in development programs. Groundwater and surface water are excellent sources of drinking water supply, especially in arid and semi-arid areas. There are significant economic advantages to their exploitation, as they require little and sometimes no processing. However, maintaining this relative advantage requires that measures be taken to sustainably preserve the quality of this resource. The Essaouira basin belongs to areas with a semi-arid climate with very irregular temperatures and precipitation in space and time that do not exceed annual averages of 20 °C and 300 mm, respectively. The decrease in precipitation due to climate change, the overexploitation of surface and groundwater due to population growth, and the continuous degradation of water quality by the intrusion of seawater bodies and by natural salinity have disturbed the stability of these resources and threatened the socioeconomic and environmental balance in the investigated area. Climate scenarios, Regional Climate Model (RCM) estimate that precipitation will decrease by 10–20% while warming increases by 3 °C in the next 30 years. Without immediate intervention, the situation will increasingly jeopardize water security in the Essaouira region.

This study concerned the qualitative and quantitative investigation of the waters of the Essaouira region (Morocco) by combining hydrochemical, GIS, and remote sensing techniques.

The research work of this article focused on the qualitative and quantitative study of surface and groundwater, the aim of which was to understand their behavior, as well as their spatiotemporal evolution. The physicochemical data used came from the 2017, 2018,

2019, and 2020 sampling campaigns. Stability in hydrogen potentials (pH) (around 7.5) and temperatures (around 23.2 °C) of the water was observed by comparing the results of the 2020 campaign with those of the former campaigns. For the electrical conductivities, a remarkable increase going from 2017 to 2020 in all the study territory was found, especially in the northern part of Ouazi, the region of Meskala, and the western border, which sometimes produced a 100% increase. Groundwater level monitoring and rainfall series over 38 years showed a decreasing trend in both variables.

A hydrogeochemical approach revealed that the groundwater mineralization was controlled by (i) the dissolution of evaporite minerals (halite and gypsum) and carbonate minerals (dolomite), (ii) the cation exchange processes, and (iii) seawater contamination. The groundwater quality for drinking purposes was evaluated and the consumption of groundwater in the study area requires treatment before use as drinking water. Regarding irrigation purposes, groundwater in the study area was suitable for plants supporting high salinity.

The processing of LandSat satellite images from TM and OLI sensors and the application of the NDWI index for a period of 14 years using GIS tools showed a slight increase in water surfaces, which was mainly explained by the commissioning of two large dams.

Author Contributions: Conceptualization: A.R.; methodology, software, validation, field investigation, resources, and data curation: A.R., M.B., A.B. and S.O.; writing—original draft preparation: A.R.; writing—review and editing, visualization, and supervision: M.B., S.O., A.B., D.O., A.C. and D.D. All authors have read and agreed to the published version of the manuscript.

Funding: This research received no external funding.

Institutional Review Board Statement: Not applicable.

Informed Consent Statement: Not applicable.

Data Availability Statement: The data presented in this study are available on request from the corresponding author.

Acknowledgments: The authors are grateful to the Editor-in-Chief of *Water* and the anonymous reviewers. The authors would also like to thank Aziz Soulaimani, the technical manager of the Water, Soil, and Plant Analysis Laboratory of the Experimental Farm at Mohammed VI Polytechnic University of Benguerir from Morocco.

Conflicts of Interest: The authors declare no conflict of interest.

References

1. Galego Fernandes, P.; Carreira, P.M.; Bahir, M. Mass balance simulation and principal components analysis applied to groundwater resources: Essaouira basin (Morocco). *Environ. Earth Sci.* **2010**, *59*, 1475–1484. [CrossRef]
2. Carreira, P.M.; Bahir, M.; Ouhamdouch, S.; Fernandes, P.G.; Nunes, D. Tracing salinization processes in coastal aquifers using an isotopic and geochemical approach: Comparative studies in western Morocco and southwest Portugal. *Hydrogeol. J.* **2018**, *26*, 2595–2615. [CrossRef]
3. Samir, K.; Younes, H.; Chkir, N.; Zouari, K. The hydro geochemical characterization of ground waters in Tunisian Chott's region. *Environ. Geol.* **2008**, *54*, 843–854.
4. Kammoun, S.; Trabelsi, R.; Re, V.; Zouari, K.; Henchiri, J. Groundwater quality assessment in semi-arid regions using integrated approaches: The case of Grombalia aquifer (NE Tunisia). *Environ. Monit. Assess.* **2018**, *190*, 87. [CrossRef] [PubMed]
5. Bahir, M.; Ouhamdouch, S.; Carreira, P.M. Isotopic and geochemical methods for studying water–rock interaction and recharge mode: Application to the Cenomanian–Turonian and Plio-Quaternary aquifers of Essaouira Basin, Morocco. *Mar. Freshw. Res.* **2018**, *69*, 1290–1300. [CrossRef]
6. Ouhamdouch, S.; Bahir, M.; Carreira, P.M.; Zouari, K. Groundwater Responses to Climate Change in a Coastal Semi-arid Area from Morocco; Case of Essaouira Basin. In *Groundwater and Global Change in the Western Mediterranean Area. Environmental Earth Sciences*; Calvache, M.L., Duque, C., Pulido-Velazquez, D., Eds.; Springer International Publishing: Cham, Switzerland, 2018; pp. 253–260. [CrossRef]
7. Ouhamdouch, S.; Bahir, M.; Carreira, P. Impact du changement climatique sur la ressource en eau en milieu semi-aride: Exemple du bassin d'Essaouira (Maroc). *Rev. Sci. l'eau J. Water Sci.* **2018**, *31*, 13–27. [CrossRef]
8. Lyazidi, R.; Hessane, M.A.; Moutei, J.F.; Bahir, M.; Ouhamdouch, S. Management of water resource from semiarid area by elaborating database under GIS: Case of Gareb-Bouareg aquifer (Rif, Morocco). *Arab. J. Geosci.* **2019**, *12*, 352. [CrossRef]

9. Bahir, M.; Mennani, A. Problematique de la gestion des eaux souterraines au Maroc. *Estudios Geol.* **2002**, *58*, 103–108. [CrossRef]
10. Boughariou, E.; Bouri, S.; Khanfir, H.; Zarhloule, Y. Impacts of climate change on water resources in arid and semi-arid regions: Chaffar Sector, Eastern Tunisia. *Desalin. Water Treat.* **2014**, *52*, 2082–2093. [CrossRef]
11. Hamed, Y.; Hadji, R.; Redhaounia, B.; Zighmi, K.; Bâali, F.; El Gayar, A. Climate impact on surface and groundwater in North Africa: A global synthesis of findings and recommendations. *Eur. Mediterr. J. Environ. Integr.* **2018**, *3*, 25. [CrossRef]
12. Alibou, J.; (Ecole Hassania Des Travaux Public, Casablanca, Morocco). Impacts Des Changements Climatiques sur Les Ressources en Eau et les Zones Humides du Maroc. Personal communication, 2002.
13. IPCC. Climate change 2013: The physical science basis. In *Contribution of Working Group I to the Fifth Assessment Report of the Intergovernmental Panel on Climate Change*; Stocker, T.F., Qin, D., Plattner, G.K., Tignor, M., Allen, S.K., Boschung, J., Nauels, A., Xia, Y., Bex, V., Midgley, P.M., Eds.; Cambridge University Press: New York, NY, USA, 2013.
14. Bahir, M.; Carreira, P.; Da Silva, M.O.; Fernandes, P. Caractérisation hydrodynamique, hydrochimique et isotopique du système aquifère de Kourimat (Bassin d'Essaouira, Maroc). *Estudios. Geol.* **2008**, *64*, 61–73.
15. Bahir, M.; Ouhamdouch, S.; Carreira, P.M. La ressource en eau au Maroc face aux changements climatiques; cas de la nappe Plio-Quaternaire du bassin synclinale d'Essaouira. *Comun. Geol.* **2016**, *103*, 35–44.
16. Ouhamdouch, S.; Bahir, M.; Ouazar, D.; Carreira, P.M.; Zouari, K. Evaluation of climate change impact on groundwater from semi-arid environment (Essaouira Basin, Morocco) using integrated approaches. *Environ. Earth Sci.* **2019**, *78*, 449. [CrossRef]
17. Bahir, M.; Ouhamdouch, S.; Ouazar, D.; El Moçayd, N. Climate change effect on groundwater characteristics within semi-arid zones from western Morocco. *Groundw. Sustain. Dev.* **2020**, *10*, 1–15. [CrossRef]
18. Bahir, M.; Ouazar, D.; Ouhamdouch, S. Dam effect on groundwater characteristics from area under semi-arid climate: Case of the Zerrar dam within Essaouira basin (Morocco). *Carbonates Evaporites* **2019**, *34*, 709–720. [CrossRef]
19. Saadi, M.; Hilali, E.A.; Bensaid, M.; Boudda, A.; Dahmani, M. Carte géologique du Maroc, échelle 1/1 000 000. *Notes Mem. Serv. Geol.* **1985**, 260.
20. Duffaud, F. Contribution à l'étude stratigraphique du bassin secondaire du Haut Atlas Occidental (Sud-Ouest du Maroc). *Bull. Soc. Géol. Fr.* **1960**, *7*, 728–734. [CrossRef]
21. Chkir, N.; Trabelsi, R.; Bahir, M.; Hadj Ammar, F.; Zouari, K.; Chamchati, H.; Monteiro, J.P. Vulnérabilité des ressources en eaux des aquifères côtiers en zones semi-arides-Etude comparative entre les bassins d'Essaouira (Maroc) et de la Jeffara (Tunisie). *Commun. Geol.* **2008**, *95*, 107–121.
22. Jalal, M.; Bahir, M.; Mennani, A. Pollution nitratée des eaux souterraines du bassin synclinal d'Essaouira (Maroc) (Nitrate in groundwater of the Essaouira Synclinal Basin, Morocco). *J. Environ. Hydrol.* **2001**, *9*, 1–10.
23. Gao, B. NDWI-A normalized difference water index for remote sensing of vegetation liquid water from space. *Remote Sens. Environ.* **1996**, *58*, 257–266. [CrossRef]
24. Bahir, M.; Ouhamdouch, S. Groundwater quality in semi-arid environments (Essaouira Basin, Morocco). *Carbonates Evaporites* **2020**, *35*, 41. [CrossRef]
25. Bahir, M.; Ouhamdouch, S.; Ouazar, D.; Chehbouni, A. Global warming and groundwater from semi-arid areas: Essaouira region (Morocco) as an example. *SN Appl. Sci.* **2020**, *2*, 1245. [CrossRef]
26. Mann, H.B. Nonparametric Tests against Trend. *Econometrical* **1945**, *13*, 245–259. [CrossRef]
27. Kendall, M.G. Multivariate Nonparametric Tests for Trend in Water Quality. *Water Resour. Bull.* **1975**, *24*, 505–512.
28. Bremond, R.; Vuichard, R. *Paramètres de la Qualité Des Eaux, Ministère de la Protection de la Nature et de L'environnement*; SPEPE: Paris, France, 1973; 179p.
29. WHO. *Guidelines for Drinking Water Quality*, 4th ed.; WHO Library Cataloguing-in-Publication Data; WHO: Geneva, Switzerland, 2011; 564p, ISBN 978 924 154815 1.
30. Piper, A.M. A graphic procedure in the geochemical interpretation of water analyses. *Trans. AGU* **1954**, *25*, 914–923.
31. Wilcox, L.V. *Classifcation and Use of Irrigation Waters*; US Department of Agriculture: New York, NY, USA, 1955.
32. Richards, L.A. Diagnosis and improvement of saline and alkali soils. *LWW* **1954**, *78*, 154. [CrossRef]
33. Gupta, I.; Salunkhe, A.; Rohra, N.; Kumar, R. Groundwater quality in Maharashtra, India: Focus on nitrate pollution. *J. Environ. Sci. Eng.* **2011**, *53*, 453–462.